Multi-Batch Micro-Selfassembly via Controlled Capillary Forces

Xiaorong Xiong[1], Yael Hanein[1], Weihua Wang[2], Daniel T. Schwartz[2], Karl F. Böhringer[1]
University of Washington
[1]Dept. of Electrical Engineering [2]Dept. of Chemical Engineering
Box 352500, Seattle, WA 98195-2500
karl@ee.washington.edu

Abstract
Recent advances in silicon processing and microelectromechanical systems (MEMS) have made possible the production of very large numbers of very small components at very low cost in massively parallel batches. Assembly, in contrast, remains a mostly serial (i.e., non-batch) technique. In this paper, we argue that *massively parallel selfassembly of microparts* will be a crucial enabling technology for future complex microsystems. As a specific approach, we present a technique for assembly of multiple batches of microparts based on capillary forces and controlled modulation of surface hydrophobicity. We derive a simplified model that gives rise to geometric algorithms for predicting assembly forces and for guiding the design optimization of selfassembling microparts. Promising initial results from theory and experiments and challenging open problems are presented to lay a foundation for general models and algorithms for selfassembly.

Keywords
Selfassembly, microassembly, massively parallel assembly, sensorless and distributed manipulation, hydrophobic, hydrophilic, capillary force.

1 Introduction
The production of silicon integrated circuits (ICs), with its capability of massively parallel batch fabrication and ever-increasing miniaturization, has been a key ingredient for the success of information technology. As a by-product, the microelectronics industry has created a vast collection of sophisticated tools and techniques to master the production of immensely complex circuits at the micro scale (approximately $10^{-3} – 10^{-6}$ m).

For more than a decade, these tools have been increasingly employed in novel ways to build microdevices that are partially or completely non-electronic, giving rise to the field of microelectromechanical systems (MEMS). Early successes were integrated pressure sensors, microfabricated print heads [1], accelerometers, and air bag sensors [2]. In the past years, micromechanical components for wireless transceivers (see, e.g., [3, 4]), micro filters and switches for all-optical networks [5], and display chips for digital projection systems [6, 7] have received much attention. Other important application areas of MEMS are gene analysis chips and biomedical microdevices [8, 9].

As the above examples show, complex heterogeneous microsystems that integrate sensing, actuation, computation, and communication in millimeter-sized volumes have become possible, inspiring concepts such as "ubiquitous or invisible computing" [10] and "smart dust" [11]. The former promises connectivity to computing and networking infrastructure at virtually any time and place. The latter envisions networks of sensing and processing "motes" that provide detailed and distributed information from virtually anywhere. The underlying idea in both cases is the extensive use of inconspicuous devices embedded in the surroundings. Possible applications include navigation and guidance systems, sensors embedded in the structural material of buildings or engines for early failure detection, or microsensors delivered from airplanes for reconnaissance.

Two features distinguish these systems from a conventional computing infrastructure:

- The combination and integration of computation with a "physical" aspect (sensing, actuation, data transmission) in self-contained microsystems.
- The distributed, massively parallel architecture with extremely large numbers of individual units.

To realize any of these systems, major challenges must be solved, including novel communications protocols, control strategies, supply of power, and the mass production of complex heterogeneous microsystems that integrate sensing, actuation, computation, and communications capabilities.

This paper focuses on the last item. Here, the challenge is the production of *very large numbers* of *heterogeneous microsystems*. Part numbers in the millions or billions may be desirable. E.g., an envisioned HTDV display made of pixels that are applied to a surface via a "smart paint" would require many millions of units. Each pixel would include a light modulator, a transceiver, and signal processing circuitry.

We pose the question: *What techniques can be devised*

that can achieve efficient assembly of microscale components, and that can be scaled up to millions or billions of parts?

Conventional pick-and-place assembly techniques are not applicable for this scenario. Instead, an approach that allows massive parallelism and open-loop control is favorable [12]. Thus, our goal is parallel micro selfassembly.

The next section discusses prior work related to selfassembly. Section 3 outlines a specific approach to microselfassembly. Its technical details and experiments are presented in Section 4, and a computational model is given in Section 5. The last sections outline initial work on algorithms for automated design optimization of selfassembling microstructures and currently open problems.

2 Related Work

The goal of obtaining complex assemblies in a self-organizing process might, at first sight, seem ludicrous. However, all chemical compounds, and all life on Earth can be considered the product of selfassembly processes.

Researchers in robotics and assembly automation have made various attempts towards employing selfassembly strategies, including early work by von Neumann and Penrose on self-organizing "assemblers" [13, 14], "shake-and-make" assemblies by Moncevicz et al. [15], and mechanical catalysts for selfassembly by Hosokawa et al. [16]. Arguably the most successful system in this category so far is SONY's APOS, which uses vibrating trays with shape-matching cutouts to position parts accurately during parts feeding [17].

By definition, selfassembly succeeds open-loop, i.e., without control via sensor feedback. Sensorless manipulation has been studied since Erdmann and Mason's tray-tilting parts feeder [18] and has been extended to parallel jaw grippers [19], conveyor belts [20], and actuator arrays at the macro and micro scale (e.g., [21-24]).

Important innovations inspired from chemistry were introduced by Whitesides and co-workers who used selfassembly driven by capillary forces and hydrophobic/hydrophilic surface interactions for simple electrical circuits [25], and recently, for 3-dimensional electronic networks [26].

In the field of MEMS, Cohn et al. [27] discussed various techniques for parallel selfassembly, and he described a first (optimistic) analysis of expected yield and assembly time based solely on thermodynamic analogies [28]. Yeh and Smith demonstrated selfassembly of pyramidal silicon blocks in shape-matching substrates [29] (in analogy to APOS at the micro scale, this technique is currently employed for SmartCards displays). Srinivasan built on Whitesides' work to demonstrate fluidic selfassembly of micro mirror arrays with sub-micron alignment precision [30, 31].

This paper makes an attempt to combine some of the key results from this broad and diverse body of research. We combine strategies based on the theory of sensorless manipulation and the batch MEMS fabrication processes with the goal to obtain a generic, widely applicable approach to parallel selfassembly.

3 Approach

The desired selfassembly process is summarized in Figure 1. Multiple *batches*, each consisting of a large number of identical *parts*, are applied in sequence. These parts collect at *binding sites* on a *substrate* in the desired arrangement without sensor feedback and in parallel. For each batch, a different set of binding sites is activated.

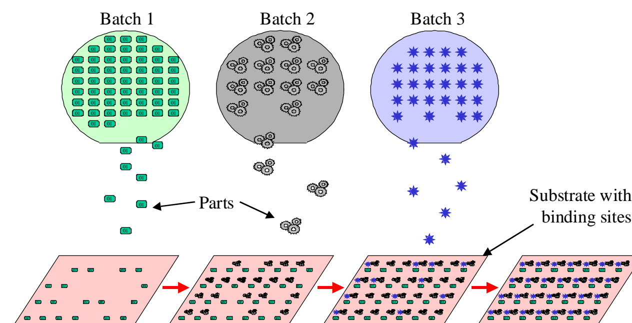

Figure 1: Multi-batch selfassembly process (conceptual drawing). In each batch, large numbers of identical parts (e.g., electronic, mechanical, and optical components) settle in parallel at predetermined binding sites on a substrate surface.

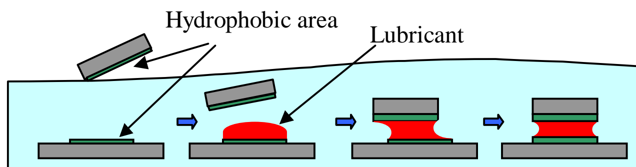

Figure 2: Hydrophobic sites on the part and the substrate cause an oil-based lubricant to form a liquid meniscus. This meniscus gives rise to the capillary forces that drive fluidic selfassembly. Note that the setup is submerged in water.

Two key questions in the realization of a selfassembly process are: (1) What is the driving force for selfassembly? (2) How can a specific assembly state be achieved? We give brief, intuitive answers in this section. The remainder of this paper will explore these issues in more detail. Note that these two questions address, respectively, the dynamics and the statics of the selfassembly process.

Binding sites. During selfassembly, microparts mate one-to-one with specific binding sites on the substrate. For multi-batch selfassembly processes, these sites must be programmable, i.e., they must permit to be activated and deactivated in a controlled manner.

Driving force. This force brings parts into alignment with their binding site on the substrate. In analogy with thermodynamics, the reduction of entropy during selfassembly requires work, which can be obtained by reduction of the system's potential energy. Our approach, building on [32, 33], uses capillary forces of a liquid meniscus between two hydrophobic sites in an aqueous solution (Figure 2).

Assembly configuration. The selfassembly process ceases once the system reaches a stable equilibrium state. Therefore, the ideal selfassembly system should be designed such that the desired assembly configuration corresponds to a unique global energy minimum, and no other local energy minima exist. Under these conditions, selfassembly represents a gradient-following descent in a physical potential field.

Since a system with only one energy minimum may be difficult to realize, local minima may be acceptable if sufficient energy can be induced to "escape" these minima, for example by random agitation. Then, selfassembly denotes an annealing process. In our system, the design of the hydrophobic binding sites determines the final assembly configuration. In Figure 2, for example, the part settles on top of the hydrophobic binding site once the capillary forces of the lubricant are in stable equilibrium.

4 Selfassembly Process

Our goal is to assemble multiple batches of microfabricated parts (size approximately 10µm – 1mm) onto a silicon wafer substrate. The liquid meniscus between hydrophobic surfaces creates the driving force for our assembly approach. The binding sites consist of lithographically patterned mating gold regions ("binding sites") coated with a hydrophobic alkanethiol selfassembled monolayer (SAM) on both substrate and parts. The SAM can be removed from gold by electrochemical reductive desorption, i.e., $CH_3(CH_2)_nSAu + e^- \rightarrow Au + CH_3(CH_2)_nS^-$ [34, 35]. Thus, the driving force can be eliminated by selectively applying a voltage bias to certain sites, which turns the gold surfaces hydrophilic. No assembly will occur in the gold regions where the SAM desorption has taken place.

Experiments: The selfassembly process consists of the following steps (see Figures 2 – 4):

- Fabrication of parts and substrate;
- SAM formation on gold surfaces of the substrate and the parts;
- desorption of SAMs from selected regions on the substrate;
- assembly of parts to the substrate sites only where no desorption has taken place.

In the last step, a hydrocarbon-based lubricant reduces friction, creates the capillary forces, and thus produces alignment between parts and substrate.

Selfassembly process details: The substrates were prepared by sputtering Cr/Au on an oxidized (100) Si wafer. The wafer was patterned with electrically isolated gold regions in a lift-off process. Then spin-on glass was patterned by photolithography and reactive ion etching (RIE) until gold squares were exposed. Test parts with sputtered Cr/Au were used. SAMs were formed on gold by immersing the substrates and the parts in 1mM ethanolic alkanethiol solution.

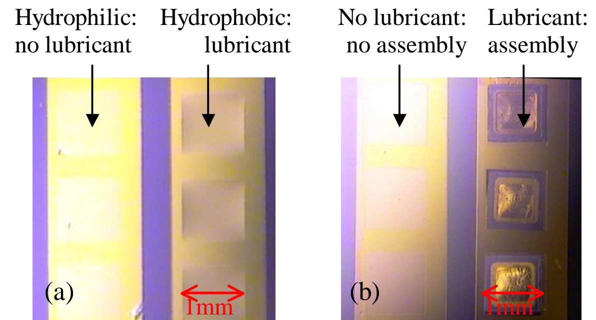

Figure 3: (a) Substrate with binding sites (square openings in transparent glass film) after selective SAM desorption. The lubricant wets only the gold squares in the right column where the SAM is still present. (b) After the first assembly step, parts are assembled only to gold patterns with adsorbed SAM and lubricant. The result after the second assembly step is shown in Figure 4.

After desorption, a hydrocarbon lubricant was spread on the substrate, which was then immersed in water. The lubricant wets only the SAM-coated hydrophobic binding sites. The differences between the gold regions with and without SAM desorption are readily seen in Figure 3a. Assembly takes place exclusively on the hydrophobic areas with lubricant. The parts were added into the water and attracted to the gold regions with the lubricant (Figure 3b). The lubricant, polymerized with heat, permanently bonded the parts to their sites. A second assembly step has been achieved by repeating the SAM formation and the assembly process. Figure 4 shows a finished two-step assembly. More details on this process can be found in [36].

The two-step selfassembly process was performed with

two different sets of $1mm^2$ chiplets. Other selfassembly experiments employed commercially available LED's and demonstrated establishing of electrical connections [36].

In principle, the process cycle of SAM adsorption, selective desorption, and controlled selfassembly can be repeated multiple times to build up increasingly complex, heterogeneous microsystems.

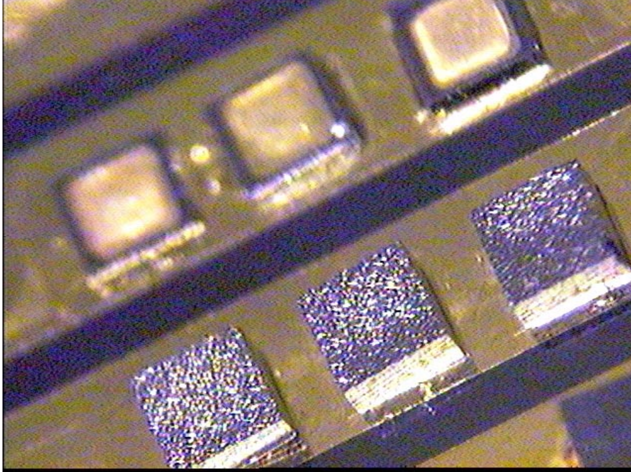

Figure 4: Side view of multi-batch selfassembly. Foreground: $1mm^2$ diced silicon chips (thickness approximately 0.5mm; unpolished backside is visible). Background: thin surface micromachined chiplets.

5 Modeling

This section investigates the forces that drive the selfassembly process and discusses a simple, computational model of capillary action. The purpose of this model is to guide the design and simulation of selfassembling systems.

Surface energy: Surface chemistry states that every interface between two liquids (or solids) has associated a surface energy. This energy derives from the ordered arrangement of molecules along the boundary layer and is responsible for phenomena such as surface tension, capillary action, and hydrophobicity. Thus, this energy is proportional to surface area; the energetically favorable state corresponds to a minimization of interfacial area (which can be observed as "surface tension"). Between water and the hydrocarbon lubricant used in our experiments, for example, this surface energy amounts to approximately γ=52 mJ/m^2 [33].

Sophisticated tools exist to model interfacial forces, and to give accurate estimates for the three-dimensional shape of fluid interfaces, contact angles, or droplet sizes (e.g., Surface Evolver [37]). However, these tools usually are based on finite element methods (FEM) and therefore computationally expensive. Thus, they are ill-suited as an evaluation subroutine during the analysis and design optimization of a selfassembly system.

A greatly simplified model was introduced recently for a liquid meniscus between two hydrophobic binding sites in close proximity in an aqueous environment [38]. Here we present a concise, more rigorous derivation of this model.

Consider again the setup described in Figure 2, which is shown in more detail in Figure 5. We are interested in the force generated by such a system that is acting on the part.

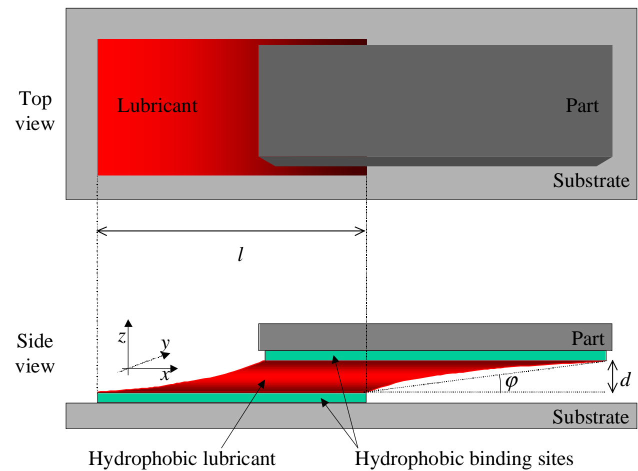

Figure 5: Top and side view of a part during fluidic selfassembly. A thin liquid film (lubricant) between the hydrophobic binding sites causes the part to align with the substrate site due to capillary forces.

It is convenient to derive this force from a straightforward energy argument. Let W be the interfacial energy of the system, and let us assume that W dominates the kinetic and potential energies of the part (this is a safe assumption for parts of less than $1mm^3$ volume in an environment with high viscous damping [39]). The general relationship between energy W and force F is given by $dW = -F\,dx$. It follows that F is proportional to the gradient in surface energy, and thus, proportional to the change in surface area of the liquid film as a function of a displacement dx.

The precise shape of the interfacial surface can be quite complicated. However, as can be seen in Figure 5, we can approximate this area from the projection of the interfacial surface onto the substrate plane. The error from this projection can be estimated by a factor $\varepsilon = \sqrt{(1+d^2/dx^2)}$. In our system, d is at most tens of micrometers, while the displacement dx is up to $l \approx$ 1mm. Thus, ε

usually lies below a few percent (but with larger errors if $dx < d$). These values are in good accordance with estimates derived from FEM analysis [40]. We conclude that as long as the separation between the binding sites is small compared to their lateral size, the projected area is a good approximation for the actual size of the interfacial surface.

Model: Let S and P be the substrate and part binding sites, respectively. The lubricant meniscus occupies a volume that, when projected onto the substrate plane, is given by $S \cup P$ (this assumes that S and P are not completely non-adjacent). Then, the projected surface M of the lubricant meniscus is $(S - S \cap P)$ and $(P - S \cap P)$, and its area can be calculated as

$$M = |S - S \cap P| + |P - S \cap P| = |S| + |P| - 2|S \cap P|. \qquad (*)$$

Interpretation: It follows from Equation (*) that the surface energy W is proportional to $M = |S| + |P| - 2|S \cap P|$. W is zero when S and P coincide perfectly. If S and P are non-adjacent, the model calculates the interfacial areas of the individual binding sites S and P. In general, W is given by

$$W = \gamma M = \gamma\,(|S| + |P| - 2|S \cap P|) \qquad (**)$$

with the proportionality factor γ (interfacial energy coefficient).

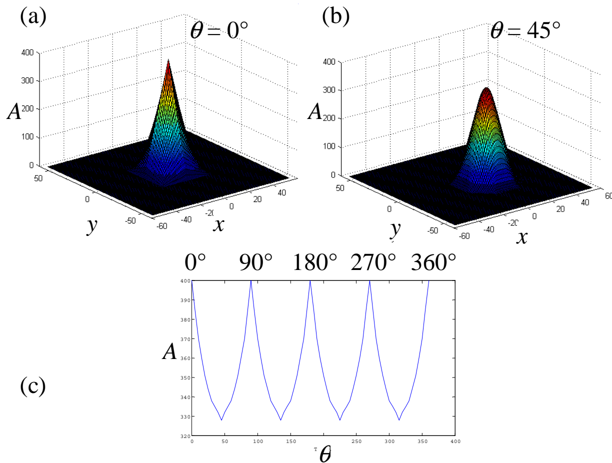

Figure 6: Surface overlap between two equal-sized squares plotted as a function of translation in x and y direction. (a) Perfect alignment between binding sites. (b) Overlap function for S and P at 45° misalignment. (c) Overlap A (maximized over all translations in x and y) plotted as function of rotation θ.

Implementation: W in Equation (**) can be broken up into a constant $W_0 = \gamma\,(|S| + |P|)$ and a factor $W' = -2\gamma\,|S \cap P|$. Thus, W' is proportional to the area overlap $A = |S \cap P|$ between S and P, which is a function of the relative position and orientation of P with respect to S. $A(x,y,\theta)$ can be calculated efficiently by the two-dimensional convolution of S and P. We call $A(x,y,\theta)$ the *area overlap function*.

6 Binding Site Design Optimization

The design of optimal binding sites for selfassembly is an important and challenging topic. Specifically, we want to determine which part and substrate binding sites ensure the highest yield and the best alignment accuracy. Since sites are usually patterned by lithography from CAD-generated masks, virtually any two-dimensional design can be implemented. We believe that the model described in the previous section is simple yet accurate enough to provide the basis for powerful computational design tools. Work in this area is still at an early stage; in the following paragraphs we briefly outline specific problems and possible approaches for algorithmic solutions.

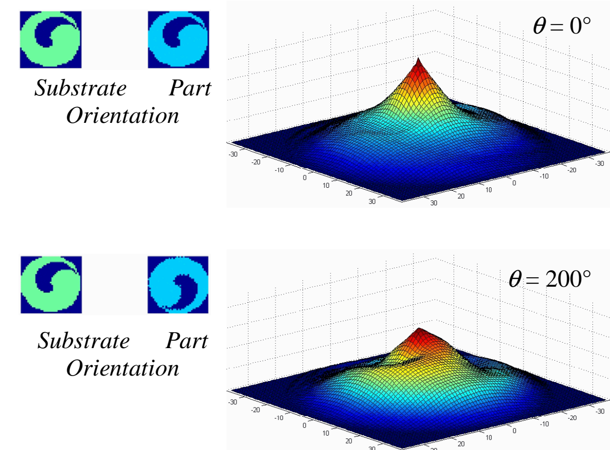

Figure 7: A design for part and substrate binding sites that exhibits only one clear global maximum. Top: Optimal alignment at 0° rotation. Bottom: lower global maximum no local maxima at 200° rotation. Design by A. Vaidya, N. Jacobson, and C. Tom.

6.1 Binding Sites for Unique Part Orientation

The design of sites that permit only one unique orientation (e.g., for selfassembly of diodes) is of particular interest. In [38], several candidate designs were investigated in simulation and experiment. However, no design with a unique selfassembly state was found. Figure 7 shows an empirically determined part design, for which simulations show only one clear global maximum for all translations and rotations (x,y,θ). However, a rigorous (non-) existence proof of designs for unique selfassembly is still pending.

6.2 Binding Sites for Given Part Designs

Often, an independent manufacturer will provide the microparts, and only the substrate binding site designs can be chosen freely.

Site design by exhaustive search. Site designs and motion in (x, y, θ) direction can be discretized to compute the overlap function $A(x, y, \theta)$, and to detect unwanted local maxima in A. A systematic search through the entire design space can then select the optimal site design.

This algorithm is demonstrated here for the simple case of one-dimensional binding sites (generalization to 2 dimensions and 3 degrees of freedom is straightforward but computationally expensive). Figure 8 shows an example site consisting of 2 hydrophobic regions (dark pixels). The algorithm generates all possible binding sites and computes the overlap function. All 9 site designs whose overlap functions have a unique global maximum (and no local minima) are listed, in descending order of maximum area overlap. Complexity of this algorithm is exponential in the resolution of the discretization.

It is interesting to note that none of the listed binding sites are exact mirror images of the part design. It is easy to see that such a site would produce local minima in the overlap function.

Another interesting observation is the fact that while the topmost binding site (the continuous hydrophobic site) results in the highest area overlap, it also produces plateaus in the overlap function. This may reduce the speed or yield of the selfassembly process, since the corresponding driving force for these configurations is zero. Other binding site designs listed below exhibit fewer plateaus.

Probabilistic design approach. To improve the expected running time of this algorithm, probabilistic search methods [41] could be employed to generate binding site designs, e.g. with genetic algorithms.

Site design via Fourier transform. We are currently studying the problem of designing a substrate site for a given part shape directly via the Fourier transform of the part design. We generate a desired energy function w with only one global minimum that corresponds to the desired assembly state. The part shape is represented by a function $p(x,y)$ that is 1 inside and 0 outside the part. We then calculate the Fourier transform of w and p, W and P, and calculate $S = W/P$, the pointwise division of W and P in the frequency domain. The inverse Fourier transform s of S then gives us a design for the substrate binding site.

Potential problems of this approach include that w is not uniquely defined, and that s needs to map into $\{0,1\}$. To circumvent these difficulties, we can a priori constrain the functions p and s to rectangular unit impulses, and thus, w to triangular impulses. Both rectangular and triangular impulses have simple representations in the frequency domain. However, a general problem with design methods based on the Fourier transform appears to be the fact that constraints such as '$w(x,y)$ must not have local minima' have no simple representation in the frequency domain.

7 Conclusions

We believe that parallel micro selfassembly is feasible and essential for the production of complex heterogeneous microsystems.

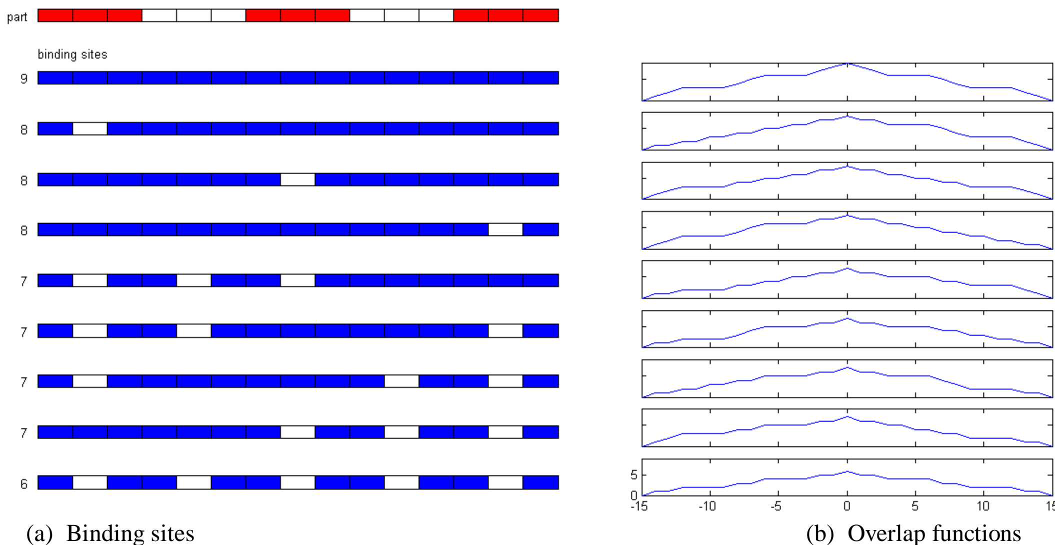

(a) Binding sites (b) Overlap functions

Figure 8: Part design and complete list of automatically generated binding sites for unique one-dimensional self-assembly. (a) The given part design is shown on top, with hydrophobic areas shown red (dark). 9 possible mating binding sites are shown below, with hydrophobic areas shown in blue (dark). (b) Overlap functions corresponding to each binding site design. All functions exhibit a unique global maximum and no local minima.

In this paper, we have demonstrated a technique for multi-batch, parallel micro selfassembly based on capillary forces and electrochemical modulation of surface hydrophobicity. It is envisioned that future microfabrication facilities will include a microassembly station where fluidic (and other) selfassembly is routinely performed as one of the production steps [42]. Current research focuses on improvement and generalization of our selfassembly technique for generic parts including standard surface mount devices, and on efficient techniques to establish electrical connections to the assembled parts.

In addition, we have derived a simple model to predict the driving forces in fluidic selfassembly based on the geometric overlap of the binding sites, and we outlined preliminary algorithms for optimization of binding site design.

Parallel micro selfassembly gives rise to a vast range of research challenges:

- Experimental: optimize yield; make process applicable to a wide range of parts and materials available in standard microfabrication processes.
- Theoretical: determine the fundamental properties and bounds of parameters such as assembly time and yield.
- Computational: develop tools for simulation and design optimization of selfassembling systems.

Selfassembly brings together the macro and the nano scale: it is influenced by chemistry and thermodynamics because of the low mass and large number of components, the dominance of surface forces, and the dependence on surface properties. Principles from assembly automation and robotics can be applied to the design and modeling of selfassembly systems, which are dominated by geometric parameters and production constraints.

Acknowledgements

We would like to thank Roger T. Howe and Uthara Srinivasan for many fruitful and inspiring discussions, and Shaoyi Jiang and Shengfu Chen for their help with surface characterization experiments. We are grateful to Les Atlas, Jeff Bilmes, Bruce R. Donald, and Hany Farid for sharing their ideas on binding site design in the frequency domain. Andreas Greiner provided valuable insights with his expertise in computational fluid dynamics and Surface Evolver. We thank the members of the University of Washington MEMS lab and the staff and users of the Washington Technology Center Microfabrication laboratory for their help and support.

This research at the University of Washington MEMS Lab was supported in part by NSF Career Award ECS-9875367 to K. Böhringer and by donations from Agilent Technologies, Intel Corporation, Microsoft Research, and Tanner Research Inc. D. Schwartz acknowledges partial support by an NSF Presidential Young Investigator Award.

References

1. Petersen, K.E., *Silicon as a Mechanical Material.* Proceedings of the IEEE, 1982. **70**(5): p. 58-95.
2. Goodenough, F., *Airbags Bom When IC Accelerometer Sees 50 g.* Electronic Design, 1991. **39**(15).
3. Mason, A., *et al.*, *A Generic Multielement Microsystem for Portable Wireless Applications.* Proceedings of the IEEE, 1998. **86**(8): p. 1733-176.
4. Nguyen, C.T.-C., L.P.B. Katehi, and R.M. Rebeiz, *Micromachined Devices for Wireless Communications.* Proceedings of the IEEE, 1998. **86**(8): p. 1756-1768.
5. Muller, R.S. and K.Y. Lau, *Surface-Micromachined Microoptical Elements and Systems.* Proceedings of the IEEE, 1998. **86**(8): p. 1705-1720.
6. Kessel, P.F.v., *et al.*, *A MEMS-based Projection Display.* Proceedings of the IEEE, 1998. **96**(8): p. 1687-1705.
7. Solgaard, O., F.S.A. Sandejas, and D.M. Bloom, *Deformable Grating Optical Modulator.* Optics Letters, 1992. **17**: p. 688-690.
8. Mastrangelo, C.H., M.A. Burns, and D.T. Burke, *Microfabricated Devices for Genetic Diagnostics.* Proceedings of the IEEE, 1998. **86**(8): p. 1769-1787.
9. Desai, T.A., *et al.*, *Nanopore Technology for Biomedical Applications.* Biomedical Microdevices, 1999. **2**(1): p. 11-40.
10. Norman, D.E., *The Invisible Computer.* 1999: MIT Press. 320.
11. Kahn, J.M., R.H. Katz, and K.S.J. Pister. *Mobile Networking for Smart Dust.* in *ACM/IEEE Intl. Conf. on Mobile Computing and Networking (MobiCom 99).* 1999. Seattle, WA.
12. Böhringer, K.F., R.S. Fearing, and K.Y. Goldberg, *Microassembly*, in *The Handbook of Industrial Robotics*, S. Nof, Editor. 1999, John Wiley & Sons. p. 1045-1066.
13. Penrose, L.S., *Self-reproducing machines.* Scientific American, 1959. **200**(6): p. 105-114.
14. von Neumann, J., *Theory of Self-Reproducing Automata.* 1966, Illinois: Un. of Illinois Press.
15. Moncevicz, P.H., Jr., M.J. Jakiela, and K.T. Ulrich. *Orientation and insertion of randomly presented parts using vibratory agitation.* in *Proceedings of the ASME Flexible Assembly Systems Conference.* 1991. Miami, Florida.

16. Hosokawa, K., I. Shimoyama, and H. Miura, *Dynamics of Self-Assembling Systems - Analogy with Chemical Kinetics.* Artificial Life, 1995. **1**(4): p. 413-427.
17. Hitakawa, H., *Advanced parts orientation system has wide application.* Assembly Automation, 1988. **8**(3): p. 147-150.
18. Erdmann, M.A. and M.T. Mason, *An Exploration of Sensorless Manipulation.* IEEE Journal of Robotics and Automation, 1988. **4**(4).
19. Goldberg, K.Y., *Orienting Polygonal Parts Without Sensing.* Algorithmica, 1993. **10**(2/3/4): p. 201-225.
20. Akella, S., *et al. Planar Manipulation on a Conveyor by a One Joint Robot With and Without Sensing*. in *International Symposium of Robotics Research*. 1995.
21. Fujita, H. *Group Work of Microactuators*. in *Int. Adv. Robot Program Workshop on Micromachine Technologies and Systems*. 1993. Tokyo, Japan.
22. Böhringer, K.F., B.R. Donald, and N.C. MacDonald, *Programmable Vector Fields for Distributed Manipulation, with Applications to MEMS Actuator Arrays and Vibratory Parts Feeders.* Int. Journal of Robotics Research, 1999. **18**(2): p. 168-200.
23. Luntz, J.E., W. Messner, and H. Choset, *Discreteness Issue in Actuator Arrays*, in *Distributed Manipulation*, K.F. Böhringer and H. Choset, Editors. 2000, Kluwer Academic Publishers Group: Norwell, MA. p. 103-126.
24. Böhringer, K.F., *et al.*, *Part Orientation with One or Two Stable Equilibria Using Programmable Vector Fields.* IEEE Transactions on Robotics and Automation, 2000. **16**(2): p. 157-170.
25. Terfort, A., N. Bowden, and G.M. Whitesides, *Three-dimensional Self-Assembly of Millimetre-Scale Components.* Nature, 1997. **386**: p. 162-164.
26. Gracias, D.H., *et al.*, *Forming Electrical Networks in Three Dimension by Self-Assembly.* Science, 2000. **289**: p. 1170-1172.
27. Cohn, M.B., *et al. Microassembly Technologies for MEMS*. in *SPIE Micromachining and Microfabrication*. 1998. Santa Clara, CA.
28. Cohn, M., *Assembly Techniques for Microelectromechanical Systems*, in *Electrical Engineering and Computer Sciences*. 1997, University or California: Berkeley.
29. Yeh, H.-J.J. and J.S. Smith, *Fluidic Assembly for the Integration of GaAs Light-Emitting Diodes on Si Substrates.* IEEE Photonics Technology Letters, 1994. **6**: p. 706-708.
30. Srinivasan, U., R.T. Howe, and D. Liepmann, *Microstructure to Substrate Self-Assembly Using Capillary Forces.* ASME/IEEE Journal of Microelectromechanical Systems, 2001.
31. Srinivasan, U., *et al. Fluidic Self-Assembly of Micromirrors onto Surface Micromachined Actuators*. in *IEEE/LEOS International Conference on Optical MEMS*. 2000. Kauai, HI.
32. Tien, J., T.L. Breen, and G.M. Whitesides, *Crystallization of Millimeter-Scale Objects With Use of Capillary Forces.* Journal of the American Chemical Society, 1998. **120**: p. 12670-12671.
33. Srinivasan, U., R.T. Howe, and D. Liepmann. *Fluidic Microassembly Using Patterned Self-Assembled Monolayers and Shape Matching*. in *Transducers'99 - International Conference on Solid-State Sensors and Actuators*. 1999. Sendai, Japan.
34. Green, J.-B.D., M.T. McDermott, and M.D. Porter, *Real Time Monitoring of the Electrochemical Transformation of a Ferrocene-Terminated Alkanethiolate Monolayer at Gold via an Adhesion-Based Atomic Force Microscopic Characterization.* J. of the Am. Chemical Society, 1996. **100**: p. 13342-13345.
35. Abbot, N.L., C.B. Gorman, and G.M. Whitesides, *Active Control of Wetting Using Applied Electrical Potentials and Self-Assembled Monolayers.* Langmuir, 1995. **11**: p. 16-18.
36. Xiong, X., *et al. Controlled Part-To-Substrate Micro-Assembly Via Electrochemical Modulation of Surface Energy*. in *Transducers'01 - International Conference on Solid-State Sensors and Actuators*. 2001. Munich, Germany.
37. Brakke, K., *Surface Evolver*. 1999, Mathematics Dept, Susquehanna Un., Selinsgrove, PA 17870.
38. Böhringer, K.F., U. Srinivasan, and R.T. Howe. *Modeling of Capillary Forces and Binding Sites for Fluidic Self-Assembly*. in *IEEE MEMS'01 - International Conference on Micro Electro Mechanical Systems*. 2001. Interlaken, Switzerland.
39. Fearing, R.S. *Survey of Sticking Effects for Micro Parts Handling*. in *IROS - IEEE/RSJ International Workshop on Intelligent Robots & Systems*. 1995. Pittsburgh, PA.
40. Greiner, A., *Personal communication*. 2001, University of Freiburg, Germany.
41. Kavraki, L.E. and J.C. Latombe, *Probabilistic Roadmaps for Robot Path Planning*, in *Practical Motion Planning in Robotics: Current Approaches and Future Directions*, K. Gupta and A. del Pobil, Editors. 1998, John Wiley. p. 33-53.
42. Howe, R.T., *Personal communication*. 2001, University of California, Berkeley.